# MODEL BASED CONTROL FOR WASTE HEAT RECOVERY HEAT EXCHANGERS RANKINE CYCLE SYSTEM IN HEAVY DUTY TRUCKS

V. Grelet[1,2,3], P. Dufour[2*], M. Nadri[2], V. Lemort[3], T. Reiche[1]
[1] Volvo Trucks GTT ATR
1 av Henri Germain, 69800 Saint Priest
vincent.grelet@volvo.com, thomas.reiche@volvo.com
[2] Université de Lyon, F-69622, Lyon, France, Université Lyon 1, Villeurbanne, France CNRS,UMR 5007, LAGEP,
dufour@lagep.univ-lyon1.fr, nadri@lagep.univ-lyon1.fr
[3] Thermodynamics Laboratory – University of Liège,
Campus du Sart Tilman, B49, 4000 Liège, Belgium
vincent.lemort@ulg.ac.be
⋆ Corresponding Author

## ABSTRACT

Driven by future emissions legislations and increase in fuel prices engine, gas heat recovering has recently attracted a lot of interest. In the past few years, a high number of studies have shown the interest of energy recovery Rankine based systems for heavy duty trucks engine compounding. Recent studies have brought a significant potential for such a system in a Heavy Duty (HD) vehicle, which can lead to a decrease in fuel consumption of about 5% [Wang et al. (2011)] and reduce engine emissions. But many challenges still need to be faced before the vehicle integration. This paper presents a control strategy development for waste heat recovery Rankine based systems in heavy duty trucks. Due to the highly transient operating conditions, improving the control strategy of those systems is an important step to their integration into a vehicle. It is shown here that moving to more advanced control strategies than classical PIDs lead to some gains in terms of performance. Due to the limited availability and high operational cost of test bench, the validation of such a controller is done on a representative and previously validated model.

## 1. INTRODUCTION

Idea of recovering heat and turning it into another form of energy is not new. By having a look in the long history of engine development, it has been introduced first through turbocharger technology and in for the commercial vehicle by the turbo-compound. Those two devices, helped the manufacturers to go through more and more stringent standards in pollutant emissions and to decrease the fuel consumption.However with nowadays engines, where those systems are present, it is hard to allocate more then 45% of fuel consumption to vehicle propulsion with classical solution. In the last decades, waste heat recovery systems (WHRS) based on Rankine cycle have attracted a lot of interest [Doyle and Kramer (1979) Oomori (1993) Wang et al. (2011)] and have shown a fuel economy potential between 5 and 10%, depending on the system complexity and the application. Contrary to stationary powerplants that use the same thermodynamic principle for electricity generation, a mobile application has very dynamic operating conditions which result into long and frequent transient behavior of the heat sources available on a vehicle. For such real driving conditions, control strategies must then be used to play a major role in the system efficiency. This topic is more and more addressed [Peralez et al. (2013), Luong and Tsao (2014)] since it is the final step for a good integration of the system into a vehicle. The control system should maximize the system performance and ensure a safe operation of the latter. Maximization of the performance is usually done by strategy optimization when safe operation means tight control of the manipulated variable(s). Here, we focus only on the second criteria since optimal strategy could only be done by taking into account all subsytems of the vehicle and not the WHRS as a standalone system. As the system dynamic is mainly controlled by the heat exchangers (HEX) behavior (i.e. evaporators and condenser) [Stobart et al. (2007), Quoilin et al. (2011)] it seems really important to focus on dynamic performance of these components. Dynamic models of HEX are of two kinds: moving boundary (MB) and finite volume (FV). Both approaches have been widely used in control system design [Peralez et al. (2013), Pettit et al. (1998)] and result in a simplification of the heat recovery boiler/condenser geometry in a great extent (e.g. by representing the boiler by a straight pipe in pipe counterflow heat exchanger). The control issue tackled here deals with one key variable: the working fluid (WF) temperature before the expansion machine which should be accurately controlled by reducing the standard deviation around its set point. This paper is organized as follows, in the second section the Rankine process and the studied system are presented. Then, in the third section, developed control strategies are explained. Section four comparing the different controller implemented, on a validated simulation model [Grelet et al. (2015)]. Finally, conclusions are drawn and perspectives are opened.

## 2. RANKINE CYCLE PRINCIPLE AND STUDIED SYSTEM

### 2.1 Rankine process

The Rankine principle is shown in its temperature-entropy form in figure 1. It can be divided into four basic transformations:

- A liquid compression where the WF reaches the evaporation pressure ($1 \rightarrow 2$) by means of the pump power consumption ($\dot{W}_{in}$).
- An evaporation where the WF is heated up ($2 \rightarrow 3a$), vaporized ($3a \rightarrow 3b$) and superheated ($3b \rightarrow 3c$) by recovering heat from the heat source ($\dot{Q}_{in}$).
- An expansion where the fluid goes from the evaporation to the condensing pressure ($3c \rightarrow 4$). The pressure drop is converted by the expander into mechanical power on its shaft ($\dot{W}_{out}$).
- A condensation where the WF goes back to the liquid phase ($4 \rightarrow 1$) by giving heat to the heat sink ($\dot{Q}_{out}$).

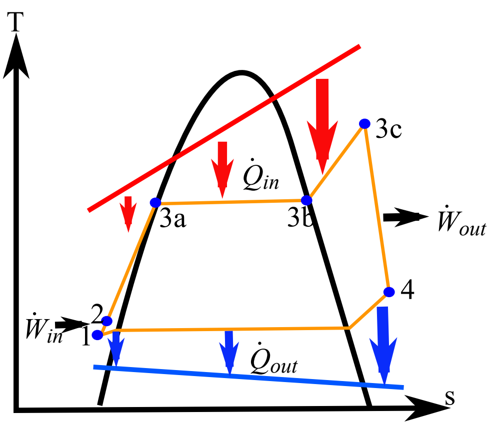


**Figure 1: Temperature-Entropy diagram of the Rankine cycle**

### 2.2 Studied system

For this application, the heat sources are the exhaust gas recirculation (EGR) and exhaust gases. The two evaporators linked to those sources are arranged in series, i.e. the WF passes first through the EGR boiler and then through the exhaust boiler. An electrical WF pump allows to control the mass flow rate in the system to achieve the control objective. The expansion machine is a kinetic turbine mechanically coupled to the engine and a liquid-cooled condenser is used to condense the WF. The WF is a water ethanol mixture showing better performance and which reduces the drawbacks of each pure fluid: freezing point of water and flammability for ethanol [Latz et al. (2012)].

## 3. CONTROLLER DEVELOPMENT

### 3.1 Control objective

As mentioned in section 1, the key parameter to control is the WF temperature before the expansion machine. This is even more critical for this system since it uses a a high speed expansion machine which is very sensitive to wet steam. Indeed, during the expansion process the droplets formation could cause erosion of the blades and damage the turbine. In order to avoid this, it seems important to have a tight control of the inlet temperature to avoid wet steam from entering into the turbine. This is usually done by turning the temperature criterion into a superheating set point (superheat corresponds to the temperature difference between present value and vapor saturation temperature) which, when positive, guarantees fully vaporized fluid entering into the expander. As the focus is on the high pressurized branch of the circuit, only the evaporators are modeled.

### 3.2 Nonlinear heat exchanger model

The modeling methodology and model validation is presented in this paper companion [Grelet et al. (2015)]. Based on finite difference scheme, The governing equations and the boundary conditions are discretized in space domain. The obtained model takes the following form (see the nomenclature at the end for the abbreviation meaning):

$$Z\dot{x}_i = f_i(x_i, u), \tag{1}$$

$$\text{where: } u = \begin{bmatrix} \dot{m}_{f,0} & P_{f,0} & h_{f,0} & \dot{m}_{g,L} & T_{g,L} \end{bmatrix}, \tag{2}$$

$$Z = \begin{bmatrix} 0 & 0 & 0 & 0 & 0 \\ 0 & 1 & 0 & 0 & 0 \\ 0 & 0 & 1 & 0 & 0 \\ 0 & 0 & 0 & 1 & 0 \\ 0 & 0 & 0 & 0 & 1 \end{bmatrix}, \tag{3}$$

$$x_i = \begin{bmatrix} \dot{m}_{f,i} & h_{f,i} & T_{w,int,i} & T_{g,i} & T_{w,ext,i} \end{bmatrix}, \tag{4}$$

$$f_i(x_i, u) = \begin{bmatrix} \dfrac{\dot{m}_{f,i-1} \frac{h_{f,i-1}}{\rho_{f,i-1}} \frac{\partial \rho_{f,i-1}}{\partial h_{f,i-1}} + \frac{1}{\rho_{f,i-1}} \frac{\partial \rho_{f,i-1}}{\partial h_{f,i-1}} \alpha_{f,i} A_{exch,int,f}\left(T_{f,i} - T_{w,int,i}\right)}{1 - \frac{h_{f,i}}{\rho_{f,i}} \frac{\partial \rho_{f,i}}{\partial h_{f,i}}} - \dot{m}_{f,i} \\ \dfrac{\left(\dot{m}_{f,i-1} h_{f,i-1} - \dot{m}_{f,i} h_{f,i}\right) - \alpha_{f,i} A_{exch,int,f}\left(T_{f,i} - T_{w,int,i}\right)}{\rho_{f,i} V_f} \\ \dfrac{\alpha_{f,i} A_{exch,int,f}\left(T_{f,i} - T_{w,int,i}\right) + \alpha_g A_{exch,int,g}\left(T_{g,i} - T_{w,int,i}\right)}{\rho_{w,int} V_{w,int}} \\ \dfrac{\dot{m}_g c_{pg}(T_{g,i})\left(T_{g,i-1} - T_{g,i}\right) - \alpha_g\left[A_{exch,int,g}\left(T_{g,i} - T_{w,int,i}\right) - A_{exch,ext,g}\left(T_{g,i} - T_{w,ext,i}\right)\right]}{\rho_{g,i} V_g c_{pg}(T_{g,i})} \\ \dfrac{\alpha_{amb} A_{exch,ext,amb}\left(T_{amb} - T_{w,ext,i}\right) + \alpha_g A_{exch,ext,g}\left(T_{g,i} - T_{w,ext,i}\right)}{\rho_{w,ext} V_{w,ext}} \end{bmatrix}. \tag{5}$$

where the ambient temperature ($T_{amb}$) is assumed constant around the entire HEX.

### 3.3 The piecewise linear approach

Developing a first principle based model is often hard (most of the parameters presented in the model (1-5) are impossible to get from experimental results) and requires a lot of effort. Using a piecewise linear model approach could be a good trade-off between controller performance and development effort. If we consider the previous model to be a single input single output (SISO) plant of the form:

$$\dot{x} = f(x, u), \tag{6}$$

$$y = g(x, u), \tag{7}$$

where $u$ is the WF mass flow entering into the EGR boiler and $y$ is the WF temperature exiting the exhaust boiler. The dynamic relation between the variation of $u$ and $y$ (also called manipulated variable (MV) and controlled variable (CV)) around an operating point can be described by a first order plus time delay

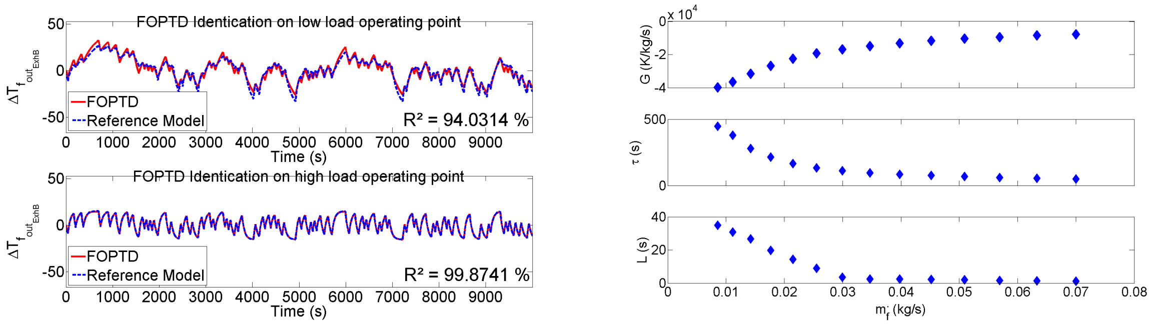


**Figure 2: FOPTD model validation (left) and parameters identified (right)**

(FOPTD) transfer function:

$$\frac{\Delta T_{f,L_{ExhB}}(s)}{\Delta \dot{m}_{f,0_{EgrB}}(s)} = \frac{G}{1+\tau s} e^{-Ds}, \tag{8}$$

where the relation between the state ($h_{f,i}$) of equation (4) and the working fluid temperature ($T_f$) can be written:

$$T_f = (a_1 P_f + a_0) h_f^2 + (b_1 P_f + b_0) h_f + (c_1 P_f + c_0), \tag{9}$$

with $a_.$, $b_.$ and $c_.$ fitted from thermodynamic database. Figure 2 shows a comparison of two different identified FOPTD model on a low and high engine load operating point and to the reference model presented in 3.2. As it can be seen on this figure the agreement is really good (94% for the low engine load point) and validates the choice of this model structure (8). The main drawback of doing this it is that FOPTD parameters varying a lot depending on the operating point where they are identified. Figure 2 shows gain, time constant and lag for the 14 identified FOPTD, hence demonstrating the nonlinearity of the system. By identifying FOPTD parameters around different relevant operating points and combining them by means of a weighting scheme a global linear model can be created. This global model is the sum of each weighted output of the $N$ identified local models. The weighting method used in this paper is based on the validity of one model among $N$, obtained by comparing the local model outputs to the plant measurements. The current (at time $k$) modeling error between the process measure and the ith model output is:

$$\varepsilon_{i,k} = y_{P,k} - y_{i,k}. \tag{10}$$

3.3.1 Bayesian estimator: State of the art adaptive estimation technique is the Bayesian estimator [Banerjee et al. (1997), Aufderheide and Bequette (2003)]. The recursive Bayesian weighting scheme is the conditional probability of the ith model present in the $N$ model bank to be true given the model population in the bank and its past history of probabilities. It assigns a weight between 0 and 1 (perfect fit of the ith model) to each model output in order to bound the global model output in the local models extreme values. The probability is calculated as follows:

$$p_{i,k} = \frac{\exp(-\frac{1}{2}\varepsilon_{i,k} K \varepsilon_{i,k}^T p_{i,k-1})}{\sum_{m=1}^{N} (\exp(-\frac{1}{2}\varepsilon_{m,k} K \varepsilon_{m,k}^T p_{m,k-1})}, \tag{11}$$

where $K$ is a convergence matrix used to accelerate the convergence to a single model and $\delta$ is an artificial small probability introduced to keep alive each model of the bank in the recursive scheme. The weight of each i[th] model is then calculated according to:

$$W_{i,k} = \begin{cases} \frac{p_{i,k}}{\sum_{m=1}^{N} p_{m,k}} & \text{for } p_{i,k} > \delta \\ 0 & \text{for } p_{i,k} < \delta \end{cases} \tag{12}$$

The two tuning parameters of this scheme are the matrix $K$ and the scalar $\delta$ and are tuned to achieved desired performance. If convergence to a single model is searched both are set relatively high whereas when more blending are wanted they are detuned and set at a low value. The global model output $\tilde{y}$ is calculated by summing the weighted local models outputs at the current time k:

$$\tilde{y}_k = \sum_{i=1}^{N} W_{i,k}\, y_{i,k} \tag{13}$$

3.3.2 New proposed estimator: In order to reduce the tuning effort and to stay as simple as possible, a new method is here proposed to compute the local models weights. All values denoted by a superscript, $\tilde{}$ , refer to normalized values.

$$\begin{aligned}
\tilde{\varepsilon}_{i,k} &= \frac{\varepsilon_{i,k}^2}{\sum_{m=1}^{N} \varepsilon_{m,k}^2}, && (14)\\
X_{i,k} &= \prod_{j\neq i, j=1}^{j=N} \tilde{\varepsilon}_{i,k}\left(1-\tilde{\varepsilon}_{j,k}\right), && (15)\\
\tilde{X}_{i,k} &= \frac{X_{i,k}}{\sum_{m=1}^{N} X_{m,k}}. && (16)
\end{aligned}$$

The value $\tilde{X}_i$ computed thanks to equation (16) is then filtered through a first order transfer function with unit static gain to obtain the current weight of each local model $W_{i,k}$:

$$W_{i,k} = \frac{1}{1+Ts}\tilde{X}_{i,k}, \tag{17}$$

where T plays the same role as the convergence matrix $K$ of equation (11), except that is a scalar instead of a matrix. The global model output is then calculated in the same way than with the Bayesian method.

$$\tilde{y}_k = \sum_{i=1}^{N} W_{i,k}\, y_{i,k}. \tag{18}$$

### 3.4 Gain scheduled PID

From the 14 identified FOPTD models, PID gains are offline computed and tabulated. These gains are then linearly interpolated function of the working fluid mass flow entering in the heat exchangers. In the rest of the study, parallel PID form are used with the addition of an anti wind-up to increase the overall performance of the controller. Gains are calculated using [Skogestad (2003)] where the tuning parameter is optimally set.

### 3.5 Nonlinear model inversion based controller

The model presented in the companion paper [Grelet et al. (2015)] and denoted by equation (1) can be reduced and inverted to be used as feed-forward term in the controller shown in figure 3. Principle and details of inversion is well explained in Peralez et al. (2013). The idea is to remove fastest dynamics in order to obtain an explicit expression of the desired MV $u$, in this case the WF mass flow ($\dot{m}_{f_0}$), function of the slowest states which are, here, the internal and external wall temperatures. Using the update of the input disturbances measure ($P_{f_0}$, $h_{f_0}$, $\dot{m}_{g_L}$, $T_{g_L}$), the system of equations defining the response of the $i^{th}$ cell of the reduced model is then:

$$\left\{\begin{array}{lcl}
0 &=& \dot{m}_f\left(h_{f_{i-1}} - h_{f_i}\right) + \dot{Q}_{f_{int_i}}\\
\frac{\partial T_{w_{int_i}}}{\partial t} &=& \dot{Q}_{f_{int_i}} + \dot{Q}_{g_{int_i}}\\
0 &=& \dot{m}_g c_{p_g}\left(T_{g_{i-1}} - T_{g_i}\right) + \dot{Q}_{g_{int_i}} + \dot{Q}_{g_{ext_i}}\\
\frac{\partial T_{w_{ext_i}}}{\partial t} &=& \dot{Q}_{g_{ext_i}} + \dot{Q}_{amb_{ext_i}}.
\end{array}\right. \tag{19}$$

The expression of the feedforward term MV $\dot{m}_f$ is then straightforward and equal to:

$$\dot{m}_f = \frac{\sum_{i=1}^{N} \dot{Q}_{f_{int_i}}}{h_{f_0} - h_{f_L}}. \tag{20}$$

The feedback part of the controller shown in figure 3 is composed of a gain scheduled PID and presented in section 3.4.

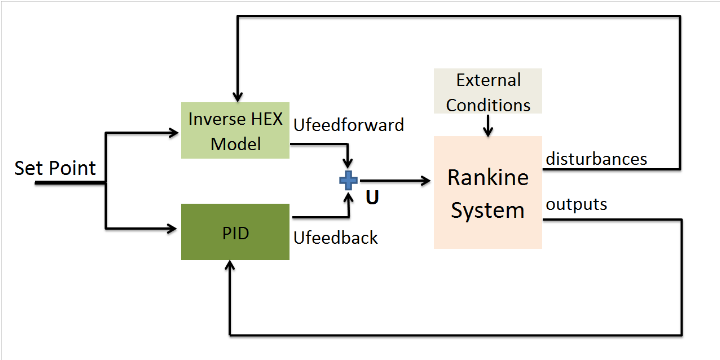


**Figure 3: Model based controller structure**

## 4. CONTROLLER PERFORMANCE

Each controller presented in section 3 is implemented under Matlab/Simulink and tested on the validated model presented in the companion paper [Grelet et al. (2015)]. A representative long haul truck driving cycle is used as simulation input (figure 4). Pump and turbine models are added to represent the high pressure part of the system.

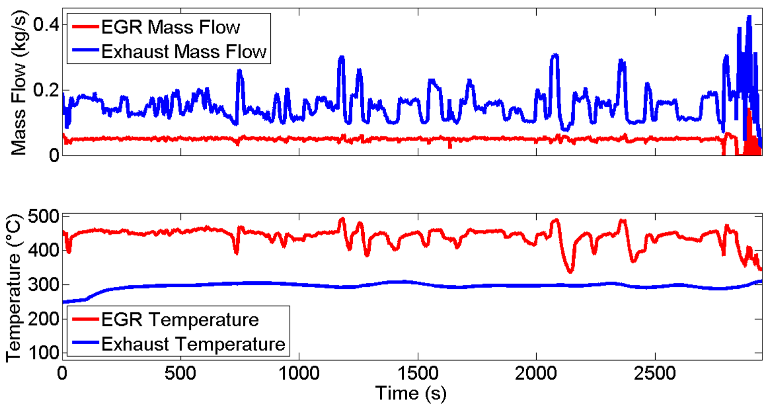


**Figure 4: Driving cycle**

### 4.1 Simulated system

The system is composed of an infinite sink at constant temperature, a first evaporator linked to the EGR gases, a second boiler recovering heat from the exhaust gases and a turbine expander. The simulated WF is composed of 20% water and 80% ethanol.

4.1.1 Pump model: The WF pump is simply represented by a fixed displacement and an isentropic efficiency. The volumetric efficiency will be a function of the outlet pressure. This law is identified thanks to experimental data.

$$\dot{m}_f = \rho_{f,in} \frac{N_{pump}}{60} C_{c_{pump}} \eta_{vol,pump} \tag{21}$$

4.1.2 <u>Turbine model:</u> The turbine nozzle is represented by the following equation:

$$\dot{m}_f = k_{eq} \sqrt{\rho_{f,in} P_{f,in} \left(1 - \frac{P_{f,in}}{P_{f,out}}^{-2}\right)}. \tag{22}$$

And the isentropic efficiency is calculated according to the following relation:

$$\eta_{is,turb} = \eta_{is,turb_{max}} \left( \frac{2c_{us}}{c_{us_{max}}} - \frac{c_{us}}{c_{us_{max}}}^2 \right), \tag{23}$$

where

$$c_{us} = \frac{u}{c_s} = \frac{\omega_{turb} R_{turb}}{2\sqrt{h_{in,turb} - h_{in,turb_{is}}}}. \tag{24}$$

Model parameters ($k_{eq}$, $\eta_{is,turb_{max}}$, $c_{us_{max}}$ and $R_{turb}$) are fitted using data from supplier.

4.1.3 <u>Actuator and sensors:</u> Pump actuator, temperature and pressure sensors are represented by first order model, fitted with data from manufacturer data.

### 4.2 Tracking performance

Controllers are compared on their ability to follow a superheat set point (SP) calculated at each time step. A set point variation is done at t = 1500s to better assess the controllers performance. Figure 5 shows the superheat tracking for the different controllers implemented.

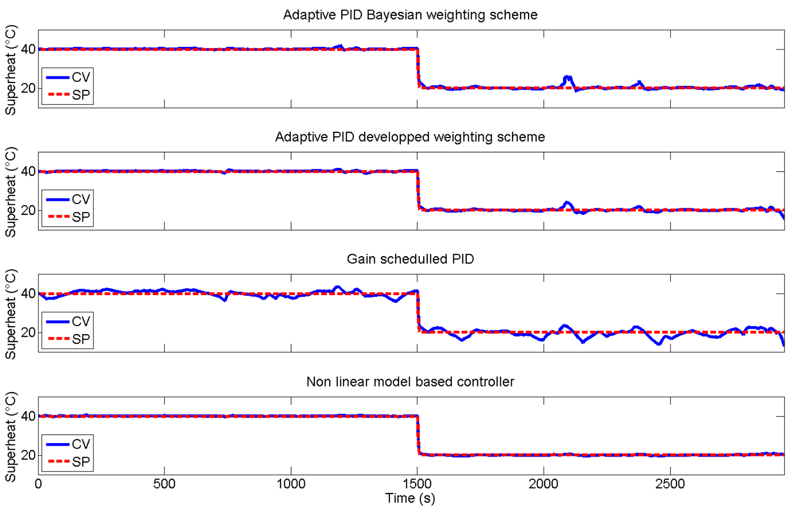


**Figure 5: Superheat tracking**

Gain scheduled PID can clearly be identified as the worst controller whereas the model based controller offers the best tracking performance. But it has to be recalled that the inverted model based control requires the perfect knowledge of all model parameter values (which is questionable), whereas the other models may be derived from various experimental process step responses. Concerning the adaptive PID, the performance is improved compared to the gain scheduling, where gains are identified off line, but it can be seen that the developed weighting scheme gives slightly better results especially when

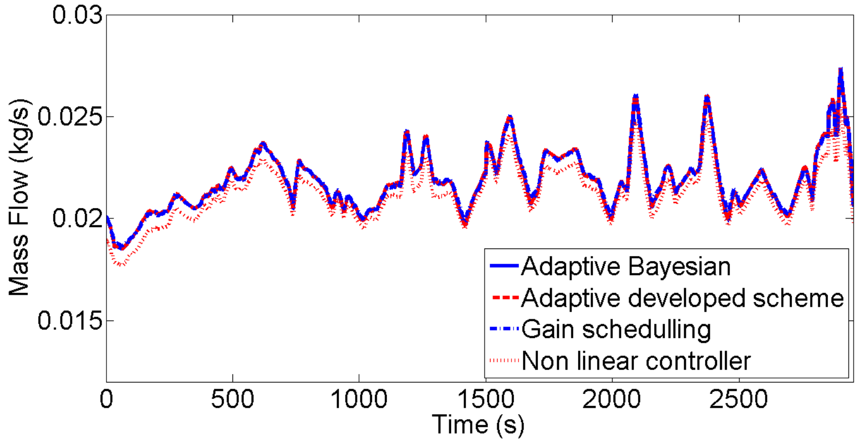


**Figure 6: Manipulated variable**

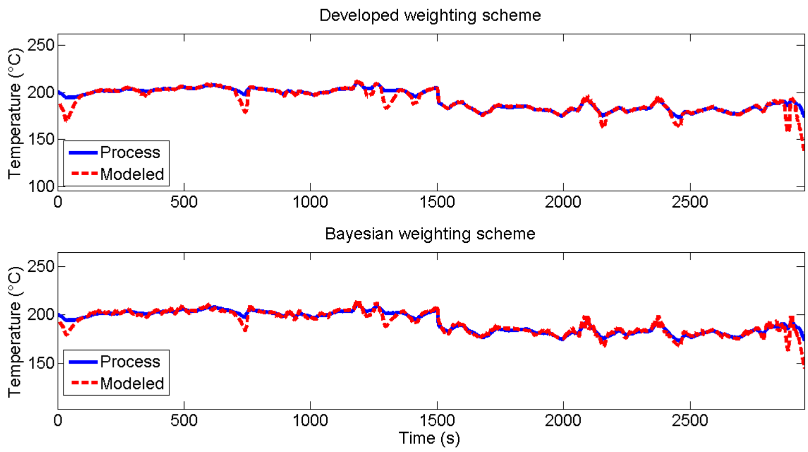


**Figure 7: Global models outputs**

large disturbances appear (at t=2200s and t=2400s). This is highlighted when looking at the integrated absolute error (*IAE*) which is a classical performance index when comparing controllers performance. It is calculated using the following relation:

$$IAE = \int_{0}^{t_{sim\ final}} |CV(t) - SP(t)| dt. \tag{25}$$

Table 1 shows the *IAE* for the four controllers. As previously said, the inverted model based controller gives the best performance, followed by the adaptive strategy with the developed weighting scheme then the Bayesian weighting scheme and the gain scheduled strategy. Moreover, there are less tuning parameters (2) in the new proposed algorithm than in the Bayesian one. The new developed strategy gives better results compared to the Bayesian weighting scheme since the transition in PID parameters is smoother. The control inputs shown on figure 6 are similar but slightly different. Figure 7 shows the outputs of the global models weighted by the two methods showed in section 3.3. The Bayesian weighting scheme gives better results but creates chattering effect due to the fast changes in weights. This could be canceled by detuning the values of the convergence matrix $K$ but not without affecting the controller performance. The developed weighting scheme includes by nature a low pass filter which avoid this effect.

| Controller | IAE |
|---|---|
| Adaptive PID with Bayesian scheme | 1044.17 |
| Adaptive PID with new proposed scheme | 958.09 |
| Gain scheduled PID | 4192.07 |
| Non linear model based controller | 417.54 |

**Table 1: Integrated absolute error for the four implemented controllers**

## 5. CONCLUSION

This study presented a new control strategy development of a waste heat recovery Rankine based system used in a long haul truck. Three different controllers are implemented and compared on a validated simulation model. Moreover, a weighting scheme for piece-wise linear approach was developed and compared to a state of the art weighting scheme. The global model outputs are similar but the developed scheme gives better results when the multi-model method is used to compute online optimal PID gains. This adaptive strategy improved significantly the performance of the PID compared to an offline gain scheduled strategy. The first principle nonlinear model based controller gave even better results but was costly in terms of development and parameter calibration, whereas the adaptive strategy requires minimum knowledge of the system and could be developed quite easily. However, the robustness of each controller still need to be investigated on an experimental setup.

## REFERENCES

Aufderheide, B. and Bequette, B. (2003). Extension of dynamic matrix control to multiple models. *Computers and Chemical Engineering*, 27(8–9):1079 – 1096.

Banerjee, A., Arkun, Y., Ogunnaike, B., and Pearson, R. (1997). Estimation of nonlinear systems using linear multiple models. *AIChE Journal*, 43(5):1204–1226.

Doyle, E. DiNanno, L. and Kramer, S. (1979). Installation of a diesel-organic rankine compound engine in a class 8 truck for a single-vehicle test. In *SAE Technical Paper*, number 790646. SAE International.

Grelet, V., Lemort, V., Reiche, T., Nadri, M., and Dufour, P. (2015). Waste heat recovery rankine cycle based system modeling for heavy duty trucks fuel saving assessment. In *3rd International Seminar on ORC Power Systems (ORC15), 2015 (Accepted)*.

Latz, G., Andersson, S., and Munch, K. (2012). Comparison of working fluids in both subcritical and supercritical rankine cycles for waste-heat recovery systems in heavy-duty vehicles. In *SAE Technical Paper*. SAE International.

Luong, D. and Tsao, T.-C. (2014). Linear quadratic integral control of an organic rankine cycle for waste heat recovery in heavy-duty diesel powertrain. In *American Control Conference (ACC), 2014*, pages 3147–3152.

Oomori, H. Ogino, S. (1993). Waste heat recovery of passenger car using a combination of rankine bottoming cycle and evaporative cooling system. In *SAE Technical Paper*, number 930880. SAE International.

Peralez, J., Tona, P., Lepreux, O., Sciarretta, A., Voise, L., Dufour, P., and Nadri, M. (2013). Improving the control performance of an organic rankine cycle system for waste heat recovery from a heavy-duty diesel engine using a model-based approach. In *52nd Annual IEEE Conference on Decision and Control (CDC)*, pages 6830–6836.

Pettit, N., Willatzen, M., and Ploug-Sørensen, L. (1998). A general dynamic simulation model for evaporators and condensers in refrigeration. part ii: simulation and control of an evaporator: Modèle général dynamique pour évaporateurs et condenseurs frigorifiques. partie ii: Simulation et régulation d'un évaporateur. *International Journal of Refrigeration*, 21(5):404 – 414.

Quoilin, S., Aumann, R., Grill, A., Schuster, A., Lemort, V., and Spliethoff, H. (2011). Dynamic modeling and optimal control strategy of waste heat recovery organic rankine cycles. *Applied Energy*, 88(6):2183 – 2190.

Skogestad, S. (2003). Simple analytic rules for model reduction and PID controller tuning. *Journal of Process Control*, 13(4):291 – 309.

Stobart, R., Hounsham, S., and Weerasinghe, R. (2007). The controllability of vapour based thermal recovery systems in vehicles. In *SAE Technical Paper*. SAE International.

Wang, T., Zhang, Y., Peng, Z., and Shu, G. (2011). A review of researches on thermal exhaust heat recovery with rankine cycle. *Renewable and Sustainable Energy Reviews*, 15(6):2862 – 2871.

## NOMENCLATURE

**Acronyms**

| | |
|---|---|
| *CV* | Controlled variable |
| *EGR* | Exhaust gas recirculation |
| *FOPTD* | First order plus time delay |
| *HD* | Heavy duty |
| *HEX* | Heat exchanger |
| *IAE* | Integrated absolute error |
| *MV* | Manipulated variable |
| *SISO* | Simple input simple output |
| *SP* | Set point |
| *WHRS* | Waste heat recovery system |

**Greek letters**

| | |
|---|---|
| $\alpha$ | Heat transfer coefficient ($W/m^2/K$) |
| $\varepsilon$ | Error (−) |
| $\eta$ | Efficiency (−) |
| $\tau$ | Time constant ($s$) |

**Latin letters**

| | |
|---|---|
| $\dot{m}$ | Mass flow ($kg/s$) |
| $\dot{Q}$ | Heat flow rate ($W$) |
| $A$ | Area ($m^2$) |
| $C_c$ | Cubic capacity ($m^3$) |
| $c_p$ | Specific heat ($J/kg/K$) |
| $D$ | FOPTD lag ($s$) |
| $G$ | FOPTD gain ($K/kg/s$) |
| $h$ | Enthalpy ($J/kg$) |
| $K$ | Bayesian recursive scheme convergence matrix (−) |
| $k_{eq}$ | Turbine throat equivalent section ($m^2$) |
| $N$ | Rotational speed ($rpm$) |
| $P$ | Pressure ($Pa$) |
| $p$ | Bayesian recursive scheme probability (−) |
| $R$ | Turbine wheel radius ($m$) |
| $T$ | Temperature ($K$) |
| $t$ | Time ($s$) |
| $V$ | Volume ($m^3$) |
| $W$ | Weight (−) |
| $X$ | Developed scheme raw weight (−) |

**Subscripts**

| | |
|---|---|
| *amb* | Ambient |
| *conv* | Convection |
| *cross* | Cross section |
| *EgrB* | EGR boiler |
| *ExhB* | Exhaust boiler |
| *exp* | Expander |
| *ext* | External wall |
| *f* | Working fluid |
| *g* | Gas |
| *in* | Inlet port |
| *int* | Internal wall |
| *k* | Current time step |
| *liq* | Liquid |
| *out* | Outlet port |
| *P* | Process |
| *sat* | Saturation |
| *vap* | Vapor |
| *w* | Heat exchanger wall |